



---

## Physicochemical Properties of Nano-Crystalline Boehmite Precipitated from Synthetic Bayer Liquor at 90 °C: Effect of Neutralization Rate

A. Krestou<sup>1\*</sup>, D. Pantias<sup>2</sup>

<sup>1</sup>Dr. Engineer, Western Macedonia University of Applied Sciences, Koila-Kozani, 50100 Greece

<sup>2</sup>Professor in the National Technical University of Athens- School of Mining and Metallurgical Engineering, 9 Heron Politechniou Str, 15780, Zografos, Greece

---

**Abstract** Boehmite is an important precursor of  $\gamma$ -Al<sub>2</sub>O<sub>3</sub> which finds many applications as catalyst and catalyst support as well as raw material for the production of adsorbents and membranes. The current work deals with the physicochemical characterization of nano-crystalline boehmite precipitated after mixing of a 2N HCl acid solution with supersaturated sodium aluminate solution at 90°C and pH7 under various mixing rates. The concentration of the supersaturated aluminate solution was chosen to simulate the concentrations of Bayer liquors that are by-products of the Bayer process. This process is the main procedure followed for the extraction of alumina from the bauxitic ore. Solutions mixing rates had a dominant effect on the microstructure of precipitates, with lower rates promoting better crystallinity of boehmite powders. An optimum mixing rate was also revealed, facilitating the highest specific surface area. The transformation temperatures of nano-crystalline boehmite precipitates to  $\gamma$ -Al<sub>2</sub>O<sub>3</sub> was found to be as low as 400°C, and was dominated by the position of adsorbed waters on the boehmite crystallites and the presence of micropores.

**Keywords** nanostructure, precipitation, Bayer liquor, catalysts

---

### Introduction

The main constituent of bauxitic ores is hydrated alumina in the form of either gibbsite ( $\gamma$ -Al(OH)<sub>3</sub>) or bayerite ( $\alpha$ -Al(OH)<sub>3</sub>), boehmite ( $\gamma$ -AlOOH) and diaspore ( $\alpha$ -AlOOH) [1]. For more than 100 years, Bayer process is the main procedure followed for the extraction of alumina from the bauxitic ore. This process consists of three consecutive main stages: a) Bauxite digestion with caustic soda; b) gibbsite, precipitation from supersaturated aluminate solution; and c) gibbsite calcination in order to produce anhydrous metallurgical grade alumina [1].

Among the hydrated aluminas, boehmite is the one with the most important technical properties since, upon heat treatment, it is transformed to a series of transition aluminas with high surface areas (200-500m<sup>2</sup>/g) and a thermal stability up to 1000°C [1,2]. Actually, upon controlled calcination boehmite undergoes a topotactic transformation to  $\gamma$ -Al<sub>2</sub>O<sub>3</sub> so that the conserved morphology and size of boehmite particles are reflected to the final transition alumina [3]. Due to their high specific surface area and thermal stability, the calcination products of boehmite are extensively used in catalytic applications either as catalysts or catalyst supports, as well as for the manufacturing of adsorbents and membranes. For this reason, many researchers have focussed their studies on the synthesis of boehmite, and especially nano-crystalline boehmite, with predetermined properties that render the material a suitable precursor for the production of transition aluminas.

In the Laboratory of Metallurgy of the National Technical University of Athens, an extensive study has been performed in order to produce boehmite rather than gibbsite from Bayer liquors. Actually, a new procedure has been developed for the synthesis of crystalline boehmite by precipitation from supersaturated sodium aluminate solutions (simulating the Bayer liquor from the primary aluminium production) under atmospheric conditions in the presence [4] and in the absence [5] of boehmite seed. In the latter case, nano-crystalline boehmite was



synthesized by titration of a  $\text{HNO}_3$  solution with a supersaturated sodium aluminate solution under a constant titration rate of 3mL/min and the proper combination of experimental conditions (temperature - pH - ageing time) were revealed in order for nano-crystalline boehmite precipitates to be formed in the temperature region 30 - 90°C. Moreover, experiments using different acids instead of  $\text{HNO}_3$ , showed that HCl is a promising acid for the precipitation of nano-crystalline boehmite with a much larger specific surface area than the one formed in the presence of  $\text{HNO}_3$  [6].

In this paper, the effect of the addition rate of supersaturated sodium aluminate solution in HCl solution on the properties that render nano-crystalline boehmite a suitable precursor for  $\gamma\text{-Al}_2\text{O}_3$  is examined at 90°C, pH7 and no ageing.

## 2. Materials and Methods

### 2.1. Materials

Pure hydrargillite ( $\text{Al}_2\text{O}_3 \cdot 3\text{H}_2\text{O}$ ) and sodium hydroxide commercially available from Merck were used for the preparation of the supersaturated sodium aluminate (SSA) solution with concentration 120g/l  $\text{Na}_2\text{O}$  and 132g/l  $\text{Al}_2\text{O}_3$ , according to the procedure found in literature [4]. Pure 2N hydrochloric acid solution was purchased by Merck chemicals.

### 2.2. Experimental procedure

The results of our previous work [5,6] showed that the addition of the SSA solution in a 2N HCl acid solution until neutralization at a rate of 3ml/min,  $T=90^\circ\text{C}$  and no ageing of precipitates in the pulp ( $t=0$ ), favoured the precipitation of pure nano-crystalline boehmite with high specific surface area ( $148,10\text{m}^2/\text{g}$ ), that was also reflected in its calcination products. In the current work, the experiments were conducted under the same experimental temperature, acidity and time of ageing by altering this time the addition rate of the SSA solution to the 2N HCl acid. Actually, a range of addition rates was examined from 1ml/min to 10ml/min. An additional experiment was also performed by the abrupt addition of a pre-calculated volume of the SSA solution to the acid at the same temperature ( $T=90^\circ\text{C}$ ), until neutralization (pH7). As soon as the acidity reached the value of pH7, the pulp was centrifuged at a speed of 2800rpm five times with distilled water and once with ethanol 99,9% [7,8] and dried at ambient temperature for two to three days.

The dried precipitates were analysed in terms of their crystallography by a SIEMENS D5000 X-Ray Diffractometer, with Ni filter and CuK $\alpha$  radiation ( $\lambda=1.5418\text{\AA}$ , 40kV, 30mA), for  $2\theta=5-80^\circ$  using a step of  $1^\circ/6,4\text{min}$ . Thermogravimetric analysis was also performed by a SETARAM LabSys instrument between 25°C and 1000°C, according to the following program: heating until 100°C, retention at this temperature for 60min, and then rise of temperature until 1000°C at a rate of 10°C/min followed by rapid cooling. The morphology of the obtained precipitates was examined by Transmission Electron Microscopy (TEM) using JEOL 2000FX and JEOL 2010F microscopes.

The specific surface area of precipitates was measured by Nitrogen adsorption at 77.3K using the BET method in a Quantachrom Nova-1200 (version 5.01) instrument. Their pore size was calculated from the desorption branch using the BJH method. Prior to adsorption, the precipitates were degassed for 20 hours at 100°C [2].

For reasons of convenience, the precipitates will be denoted hereafter as XBCI9070, where X is the SSA addition rate in ml/min ( $X=1, 3, 5, 7, 10$  and ab for abrupt addition), B for Boehmite, Cl for HCl, 90 for 90°C, 7 for pH7, and 0 for ageing time in sec.

## 3. Results and Discussion

### 3.1 Crystallographic Analysis

The crystallographic diagrams of all precipitates are given in the following Figure 1.

From Figure 1 it is obvious that the addition rate did not affect the type of precipitates, with boehmite being the only phase detected under the same experimental temperature, pH and time of ageing. The broad diffraction peaks indicated a nano-crystalline material with large amounts of amorphous phase present. This kind of boehmite is found in the literature either as nano-crystalline boehmite or pseudoboehmite [1]. From the same Figure 1 it is also evident that a rise of the addition rate resulted in a reduction of the intensity of the diffraction peaks, especially of the major [020] peak that was substantially broadened. Although the intensity reduction of



all diffraction peaks, the [200] and [002] peaks remained sharper than the [020] one, implying thin, platelet like crystallites [9].

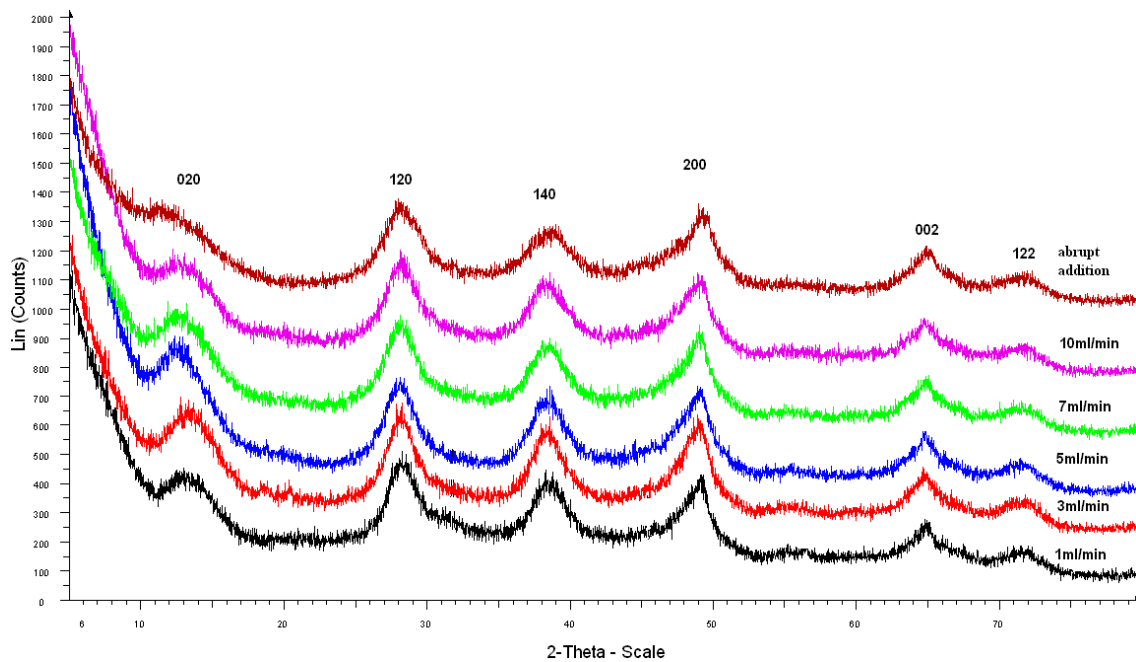


Figure 1: XRD diagrams of the AlOOH precipitates obtained under various addition rates of the SSA solution to 2N HCl, at 90°C, pH7, without ageing in the pulp. The main hkl indices of boehmite are also shown.

Scherrer formula [10] was applied in order to estimate the average crystallite size of the precipitated boehmite samples (Table 1). The estimated values were very close to the lower application limits of the Scherrer equation (application range 1-100nm) [10]. The mean crystallite size as well as the interplane distance  $d_{020}$  values for each boehmite precipitate is also presented in the same Table 1.

Table 1: Average crystallite size of the nano-crystallite boehmite precipitates

hkl	Average Crystallite size, nm					
	Addition rates					
	1mL/min	3mL/min	5mL/min	7mL/min	10mL/min	Abrupt addition
020	2,764	2,815	3,085	2,720	2,700	-
120	3,970	3,933	3,766	3,757	3,783	3,171
140	3,619	3,862	3,561	3,651	3,538	3,112
200	4,519	4,476	4,610	4,864	4,258	4,321
002	5,830	5,434	6,375	6,258	5,881	4,848
122	4,858	4,139	5,573	4,794	5,604	4,576
<b>Mean crystallite size, nm</b>	<b>4,260</b>	<b>4,110</b>	<b>4,495</b>	<b>4,341</b>	<b>4,299</b>	<b>4,004</b>
<b><math>d_{020}, \text{Å}</math></b>	<b>6,677</b>	<b>6,682</b>	<b>7,115</b>	<b>7,173</b>	<b>7,296</b>	<b>7,406</b>

The higher boehmite crystallite dimensions in the crystallographic directions [200] and [002] compared to the ones in the [020] direction (Figure 1 and Table 1) indicate that the crystallites were preferably grown on the a-c crystallographic plane, a trend that is characteristic of nanocrystalline boehmite [1]. As also presented in Table 1, the interplane distance ( $d_{020}$ ) values for all precipitates were shifted to larger values than the one corresponding to crystalline boehmite (6,1Å) [1]. Actually, as the addition rate rose from 1mL/min to abrupt addition, the  $d_{020}$  was also increased from 6,677Å to 7,406Å. These values are characteristic of pseudoboehmite (6,67Å) [11], have been also observed by other researchers [7, 11], indicate a less crystalline material and have been ascribed either to interlayer water [7, 11], or defects [11] or even to limited number of double layers [7] in the boehmite structure.



The aforementioned XRD data were also confirmed by the TEM images (Figure 2), that revealed the presence of very fine nano-crystals dispersed in an amorphous phase.

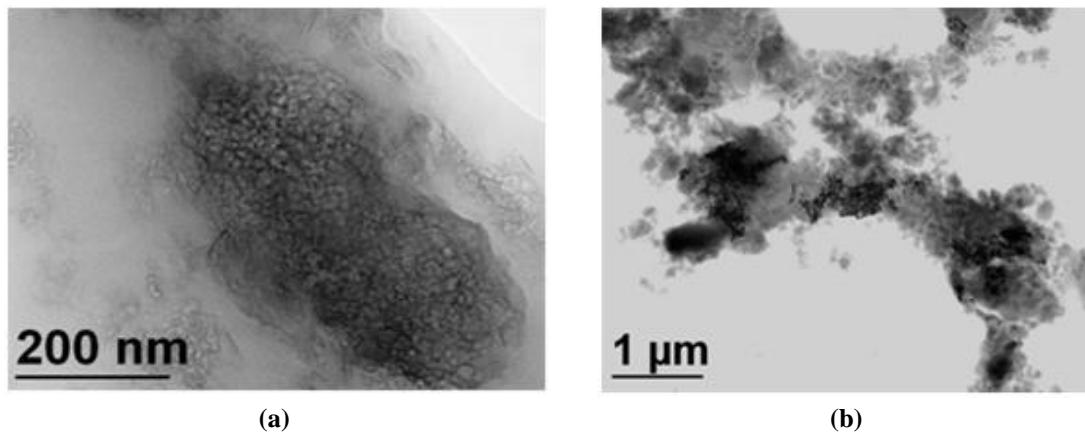
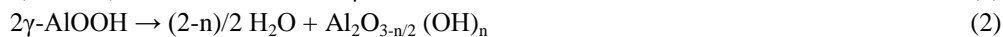


Figure 2: TEM images for samples (a) 5BCI9070 and (b) 10BCI9070. The samples seem to comprise of amorphous phase with dispersed very fine nano-crystals

From Table 1 it is also evident that a rise in the titration rate from 1 to 5mL/min resulted in a rise of the crystallites width (crystallite size on the [020] crystallographic direction) with a simultaneous rise of the interplane distance in the same direction ( $d_{020}$ ). This trend could be attributed to interlayer waters in the [020] direction, causing a “swelling” of the crystallites in this direction. On the other hand, a further rise in the titration rate (7, 10ml/min and abrupt addition) lead also to a rise in the  $d_{020}$  however the crystallite size in the same direction [020] was reduced (Table 1). The crystallite sizes of samples 7BCI9070, 10BCI9070 and abBCI9070 showed a preferable growth on the (200) and (002) planes at the expense of growth on the (020) plane. If a, b and c are the crystallite sizes on the main crystallographic growth directions of boehmite [200], [020] and [002], respectively, the c/b value for samples 1BCI9070, 3BCI9070 and 5BCI9070 is lower than the one of samples 7BCI9070 and 10BCI9070. The same trend is true for the a/b ratio. This preferable growth for the high titration precipitates 7BCI9070 and 10BCI9070 could imply the presence of high surface crystallites on which water sorption is facilitated [8, 9]. Therefore, the high values of  $d_{020}$  in the latter samples could be attributed to a limited number of double layers accompanied by the presence of chemically sorbed water on their surface.

### 3.2 Thermal analysis

The Differential Thermal Analysis (DTA) diagrams of all nano-crystalline boehmite precipitates (Figure 3), revealed two temperature regions (regions I & II) where endothermic phenomena take place. According to literature [2], the first endothermic phenomenon (region I) with a peak close to, but lower than 200°C, corresponds to the removal of physically adsorbed molecules of water as well as to the primitive dehydroxylation of boehmite according to the chemical reactions (1) and (2):



where, m and n denote the number of physically adsorbed molecules of water and the number of hydroxyl groups remaining in the dehydroxylated transition alumina respectively.

This endothermic phenomenon in region I is typical for boehmite samples with crystal sizes smaller than 50nm [2] and results in the formation of a boehmite with less water molecules and substantially better crystallinity as is seen in Figure 4 for sample 5BCI9070. As shown in the same Figure 4, the low temperature (210°C) water removal from the nano-crystalline boehmite improved substantially its crystallinity with the most evident sharpening resulting on the [020] peak, which could be attributed to the removal of the big amount of water entrapped on the (020) crystallographic plane, as previously discussed.



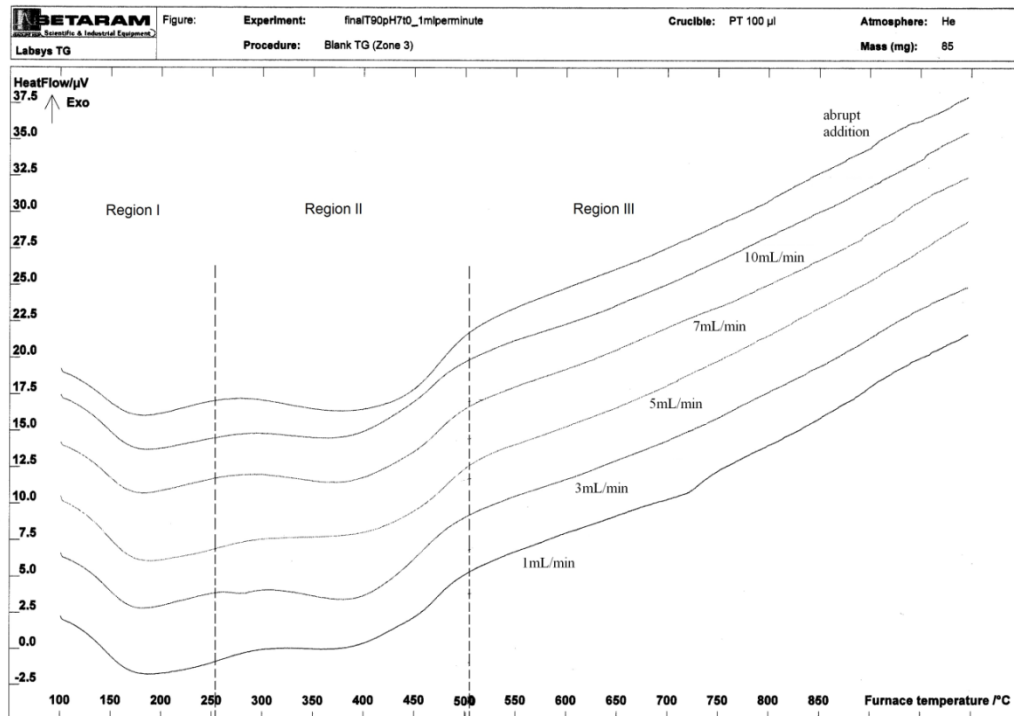


Figure 3: DTA diagrams of nanocrystalline boehmites precipitated under different addition rates

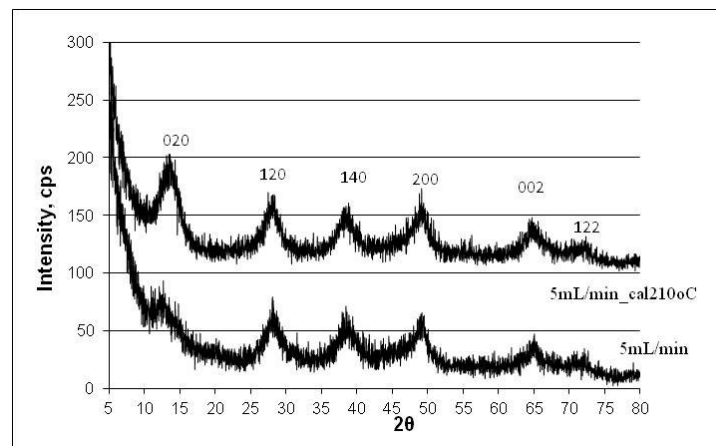


Figure 4: XRD diagrams of the 5BC19070 precipitate and its thermal treatment product at 210 °C.

The second endothermic effect close to 400°C (Region II) is characteristic of the full dehydroxylation of the transition alumina (reaction 3) which results to the transformation of nano-crystalline boehmite to  $\gamma$ -Al<sub>2</sub>O<sub>3</sub> [2].



The total mass loss for all nano-crystalline boehmite precipitates was about 19-23% (Table 2), was higher than the theoretical value (15%) calculated from equation (4)



and has been also observed from other researchers [1]. The number of water molecules per Al<sub>2</sub>O<sub>3</sub> in the structure of precipitates calculated from this mass loss was between 1.3 and 1.5 with these values being characteristic for pseudo-boehmite [12].

In Figure 5, the crystallite width (crystallite size parallel to (020) plane), the number of water molecules per Al<sub>2</sub>O<sub>3</sub> in the structure of precipitates and the value of  $d_{020}$  are plotted against the addition rate. As shown in this Figure, two discrete regions of addition rates can be observed: one for addition rates up to 5 mL/min (Region I)



and one for higher addition rates (Region II). In Region I, there is a good correlation between the crystallite width, the number of water molecules per  $\text{Al}_2\text{O}_3$  and the  $d_{020}$  value. The simultaneous rise of the crystallites width and the value of  $d_{020}$  as the addition rate increased from 1 to 5 mL/min, could be attributed to the increased number of water molecules intercalated between the double layers of boehmite structure, causing a swelling of the crystallites width and a consequent shift of  $d_{020}$  to higher values, as implied in the previous section. At higher addition rates (Region II) the correlation among the three entities did not exist. The  $d_{020}$  values continued to increase indicating that the precipitated boehmite structure became more and more amorphous with limited number of double layers. Under these conditions, the number of intercalated water molecules per  $\text{Al}_2\text{O}_3$ , the crystallite width (Figure 5) and the mean crystallite size (Table 1), decreased.

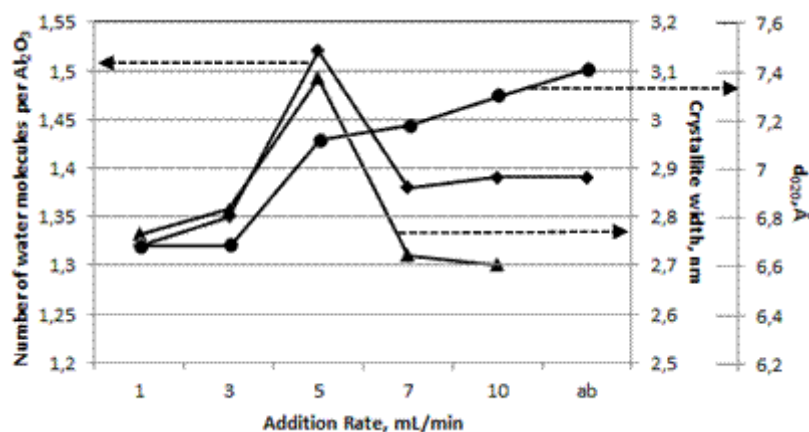
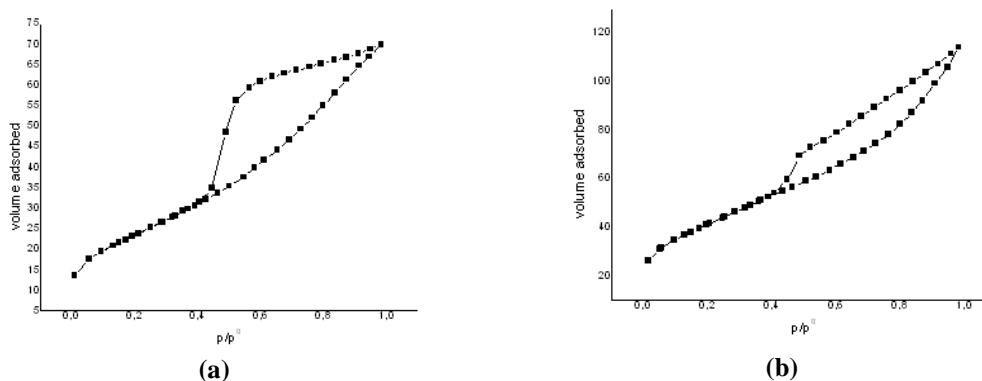


Figure 5: Effect of the addition rate on the crystallite width, the number of water molecules per  $\text{Al}_2\text{O}_3$  and on the interplane  $d_{020}$  values of precipitated nano-crystalline boehmites

### 3.3. Specific surface area

Nano-crystalline boehmite precipitates presented high specific surface areas ranging from 85 to  $170\text{m}^2/\text{g}$  as shown in Table 2. As it was expected, the precipitate with the best crystallinity (1BCI9070) presented the lowest specific surface area, since the better the crystallinity the lower the specific surface area [7].

The  $\text{N}_2$  adsorption-desorption isotherms for all samples are presented in Figure 6. The adsorption isotherm for 1BCI9070 precipitate was clearly of Type IV, which is characteristic for catalysts [13]. For all other samples, the adsorption isotherm was pseudo-Type II. The adsorption isotherm for samples 5BCI9070 and abBCI9070 seemed to be almost linear up to  $p/p^0 = 0.9$ , a feature that is indicative of the presence of micropores [13, 14]. All samples, with the exception of the 3BCI9070, showed a hysteresis loop corresponding to the IUPAC classification of Types H2 & H3 [13], which imply the presence of a network comprising of voids between agglomerated platelet like particles. The calculated specific surface area of the boehmite precipitates showed an upward trend with rise of the addition rate up to 5ml/min and then started to decrease (Table 2).



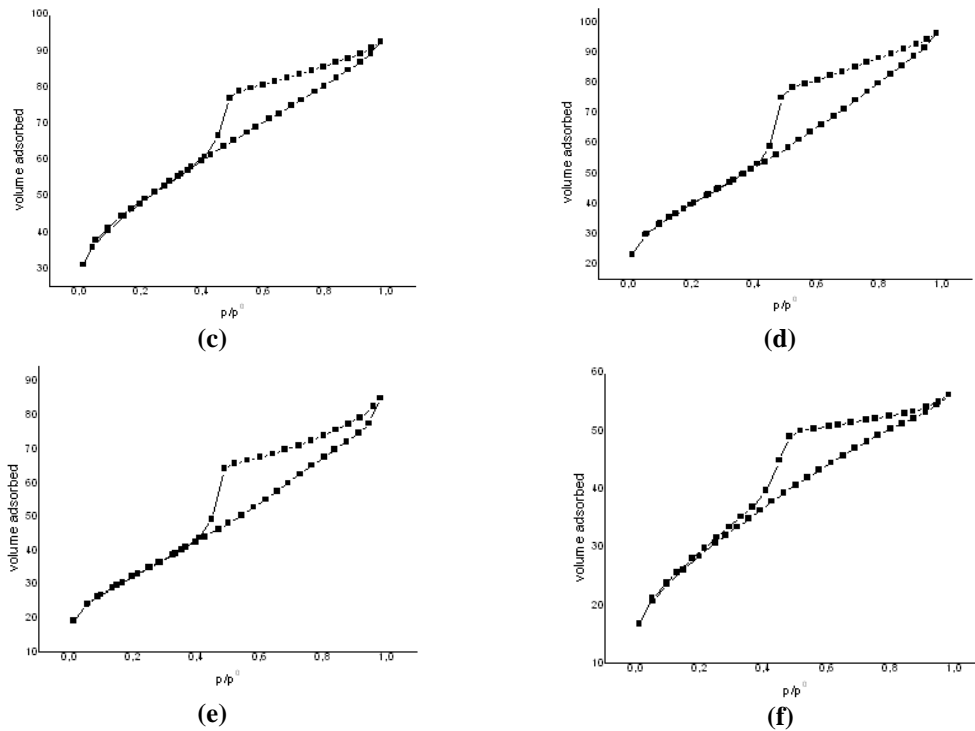
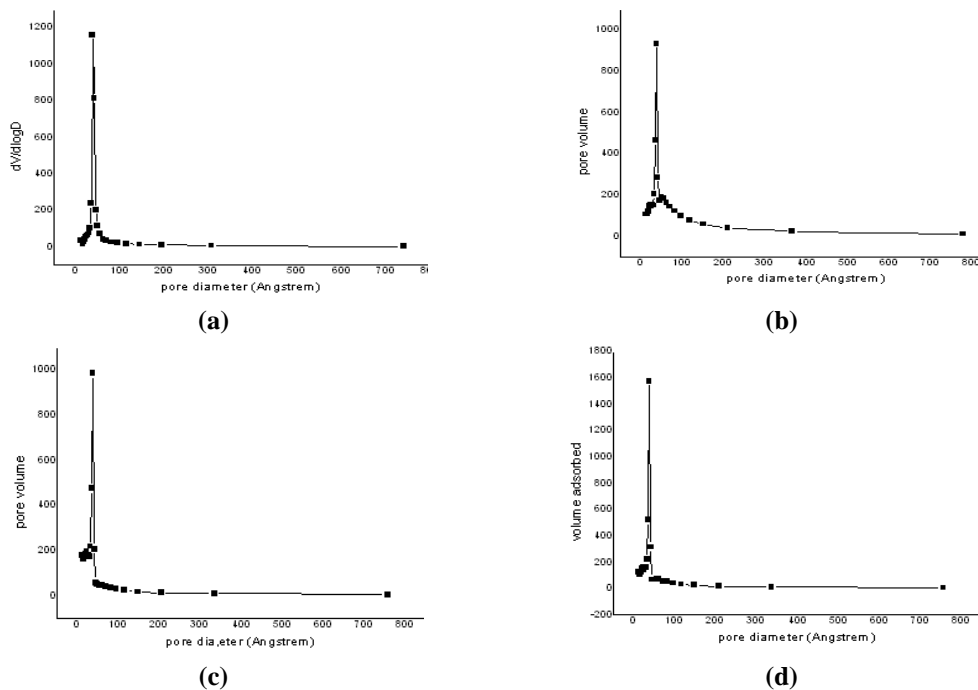


Figure 6:  $N_2$  adsorption-desorption isotherms of the nano-crystalline boehmite precipitates a) 1bCl9070, b) 3BCl9070, c) 5BCl9070, d) 7BCl9070, e) 10BCl9070 and f) abBCl9070

The mean pore diameter of all precipitates was in the mesoporous range (Table 2) and showed generally a narrow distribution in this range (20 - 200Å) without incorporation of macropores (pores with diameter higher than 200Å) as is shown in Figure 7. In the 3BCl9070 precipitate (Figure 7b), some large mesopores with diameter inbetween 100 - 200Å seemed to be present. Finally, in the 5BCl9070 and abCl9070 (Figure 7c and 7f, respectively) precipitates an incorporation of an appreciable amount of micropores with diameter lower than 20Å was evident. The same trend, but in a substantially smaller extent, was also observed for 7BCl9070 and 10BCl9070 precipitates (Figure 7d and 7e, respectively), with a higher amount micropores incorporated in the former than in the latter precipitates.



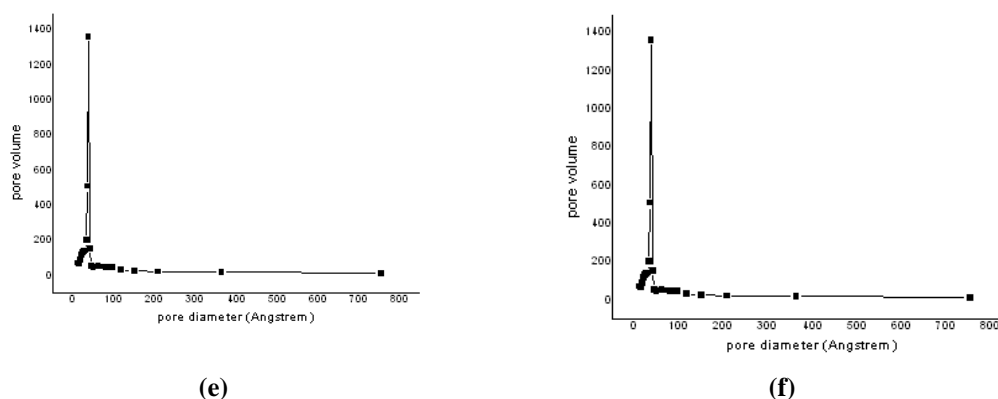


Figure 7: Pore size distribution of the nano-crystalline boehmite samples a) 1BCI9070, b) 3BCI9070, c) 5BCI9070, d) 7BCI9070, e) 10BCI9070 and f) abBCI9070

### 3.4 Transformation temperature to $\gamma$ -Al<sub>2</sub>O<sub>3</sub>

According to literature [1, 7] the transformation temperature of crystalline boehmite to  $\gamma$ -Al<sub>2</sub>O<sub>3</sub> is altered proportionally to its crystallite size, since larger crystallites require longer dehydroxylation path lengths [7]. Actually, well crystallized boehmite transforms to  $\gamma$ -Al<sub>2</sub>O<sub>3</sub> close to 470°C [1], while much lower temperatures are required for the same transformation of pseudoboehmite. Therefore, it is not surprising that the nano-crystalline boehmites in the current study transformed to  $\gamma$ -Al<sub>2</sub>O<sub>3</sub> at temperatures as low as 390°C. However, a comparison between the transformation temperatures of the nano-crystalline precipitates indicated that the smallest crystallite size (abCI9070 precipitate) did not lead to the lowest transformation temperature (Table 2, temperature in region II).

According to the literature [2], the activation energy for the transformation of nano-crystalline boehmite to transition aluminas, is close to the energy of chemisorption of H<sub>2</sub>O on  $\gamma$ -Al<sub>2</sub>O<sub>3</sub>. Therefore, the transformation of nano-crystalline boehmite to transition alumina is probably controlled by the difficulty in the removal of the chemisorbed water [2], which implies the necessity for elevated energy (higher temperatures) in order the transformation to be completed. As a result, the 5BCI9070 and abBCI9070 nano-crystalline precipitates, both containing micropores and defects in their structure (Table 2), transformed to  $\gamma$ -Al<sub>2</sub>O<sub>3</sub> at higher temperatures than the other samples, since water is chemisorbed in micropores.

The micropores can be also regarded as obstacles to the rearrangement of the atoms during the topotactic transformation of boehmite to  $\gamma$ -Al<sub>2</sub>O<sub>3</sub>, increasing the required temperature for transformation to occur. This is evident by the corresponding data of the 10BCI9070 and abCI9070 precipitates (Table 2). Although both precipitates contained the same amount of water molecules chemisorbed on their surface, the presence of micropores in the abCI9070 precipitates resulted in almost a 10°C rise of its transformation temperature to  $\gamma$ -Al<sub>2</sub>O<sub>3</sub>.

**Table 2:** Physicochemical properties of the nano-crystalline boehmites precipitated under different addition rates

	1BCI9070	3BCI9070	5BCI9070	7BCI9070	10BCI9070	abBCI9070
% Region I mass loss	9,23	9,22	11,56	8,72	8,63	7,24
% Region II mass loss	10,55	11,08	11,31	11,91	12,24	13,62
%total mass loss	19,78	20,30	22,87	20,63	20,89	20,86
number of adsorbed water molecules	1,32	1,35	1,52	1,38	1,39	1,39
T in region I, °C	185,72	187,86	191,06	183,03	186,46	164,51
T in region II, °C	393,76	396,95	407,25	394,33	387,29	398,69
ssa, m <sup>2</sup> /g	85,25	148,10	170,87	144,52	118,31	104,25
mean pore diameter, nm	5,068	4,755	3,347	4,118	4,445	3,333
pore volume, cc/g	0,11	0,18	0,14	0,15	0,13	0,09
Pores distribution	narrow in	narrow in the	narrow in the	narrow in the	narrow in	narrow in the





	the mesoporous range	mesoporous range, with some large mesopores present (10-20nm)	mesoporous range, with micropores incorporated	mesoporous range	the mesoporous range	mesoporous range, with micropores incorporated
<b>adsorption isotherm</b>	Type IV	pseudo-Type II	pseudo-Type II	pseudo-Type II	pseudo-Type II	pseudo-Type II
<b>hysteresis loop</b>	mixed Type H2 & H3	Type H3	mixed Type H2 & H3	mixed Type H2 & H3	mixed Type H2 & H3	mixed Type H2 & H3

#### 4. Conclusions

The current work showed that pure nano-crystalline boehmite can be precipitated by the neutralization of a hydrochloric acid solution using a Synthetic Bayer liquor (supersaturated sodium aluminate solution, SSA solution). Under the examined temperature, pH and ageing conditions, the only precipitate formed was nano-crystalline boehmite, the physicochemical properties of which depending on the addition rate.

All nano-crystalline precipitates presented high specific surface areas ranging from 85-170g/m<sup>2</sup>. The precipitate with the lowest specific surface area was the one formed under the lowest examined neutralization rate (1mL/min) that also presented the best crystallinity from all other precipitates. As the neutralization rate rose from 1 to 5mL/min, the specific surface area of the corresponding nano-crystalline precipitates was increased. A further rise in the neutralization rate lowered the specific surface area of the precipitates, indicating that the rate of neutralization dictated the microstructure of precipitates.

It was shown that the neutralization rate affected the amorphicity of the precipitated boehmites. Increased neutralization rates decreased the intensity of the diffraction peaks with the most evident influence being the broadening of the main boehmite [020] diffraction peak.

An increase of the SSA solution addition rate from 1mL/min to 5mL/min caused the intercalation of water molecules between the interlayers of nano-crystalline samples, swelling of the crystallites width and a continuous reduction of pore size. The precipitates formed at a neutralization rate of 5mL/min, contained the highest amount of intercalated water, while presented a defect structure as well as internal surface area, responsible for the largest specific surface area of the sample and the highest required temperature for its transformation to  $\gamma$ -Al<sub>2</sub>O<sub>3</sub>.

A further rise in the SSA solution addition rate from 7ml/min up to 10mL/min, changed the morphology of nano-boehmite crystallites, deconstructing the typical double layers structure of boehmite. Under these neutralization rates, the number of intercalated water molecules per Al<sub>2</sub>O<sub>3</sub>, the crystallite width, the mean crystallite size and the specific surface area decreased. At the same time, the mean pore diameter increased and the incorporation of micropores in the pore distribution of precipitates decreased, lowering the required transformation temperature to  $\gamma$ -Al<sub>2</sub>O<sub>3</sub>. Exception comprised the nano-crystalline boehmite precipitated after the abrupt addition of the SSA solution to the HCl solution. In these precipitates, micropores were present resulting in increased required transformation temperatures.

#### Acknowledgments

The authors would like to thank Dr. Kepaptsoglou for the TEM analysis of the samples performed in the University of Oslo.

#### References

- [1]. Wefers K., Mishra C. (1987). Oxides and Hydroxides of aluminium. *Alcoa Technical paper 19* revised, Alcoa laboratories.
- [2]. Alphonse P. and Courty M.. (2005). Structure and Thermal Behavior of Nanocrystalline Boehmite. *Thermochimica Acta*, 425:75-89.
- [3]. Raybaud P., Digne M., Iftimie R., Wellens W., Euzen P., Toulhoat H.. (2001). Morphology and Surface Properties of Boehmite ( $\gamma$ -AlOOH): A Density Functional Theory Study. *Journal of Catalysis*, 201: 236- 246.
- [4]. Skoufadis C., Panias D., Papsaliaris I.. (2003). Kinetics of boehmite precipitation from supersaturated aluminate solutions. *Hydrometallurgy*, 68 : 57-68.



- [5]. Krestou A., Panias D.. (2007). Effect of synthesis parameters on precipitation of nanocrystalline boehmite from aluminate solutions. *Powder Technology*, 175 (3): 163 - 173.
- [6]. Panias D., Krestou A.. Synthesis of nano-  $\gamma$  AlOOH from aluminate solutions for catalytic applications. *Proceedings of the 3<sup>rd</sup> International Symposium on Light Metals and Composite Materials*, 12-14 September 2008, Belgrade, Serbia: 43-52.
- [7]. Okada K., Nagashima T., Kameshima Y., Yasumori A. and Tsukada T.. (2002). Elaboration of an Easy Aqueous Sol-Gel Method for the Synthesis of Micro- and Mesoporous  $\gamma$ -Al<sub>2</sub>O<sub>3</sub> Supports. *Journal of Colloid and Interface Science*, 253: 308-314.
- [8]. Hwang K-T., Lee H-S., Chung K-C., Park S-S., Lee J-H.. (2001). Synthesis of aluminium hydrates by a precipitation method and their use in coatings for ceramic membranes. *Journal of the European Ceramic Society*, 21(3): 375-380.
- [9]. Bokhimi X., Toledo-Antonio J.A., Guzman-Castillo M.L and Hernandez- Beltran F.. (2001). Relationship between Crystallite Size and Bond Lengths in Boehmite. *Journal of Solid State Chemistry*, 159 (1): 32-40.
- [10]. Klug H. P., Alexander L. E. (1954). *X-Ray Diffraction procedures for polycrystalline and amorphous materials*, John Willey & Sons Inc.
- [11]. Petrovic R., Milonjic S., Jokanovic V., Kostic- Gvozdenovic Lj., Petrovic-Prevelic I., Janackovic Dj.. (2003). Influence of synthesis parameters on the structure of boehmite sol particles. *Powder Technology*, 133 (1-3): 185-189.
- [12]. Chuah G.K., Jaenicke S., Xu T.H.. (2000). The effect of digestion on the surface area and porosity of alumina. *Microporous and Mesoporous Materials*, 37 (3): 345-353.
- [13]. Gregg S.J. (1982). *Adsorption surface area and porosity*, Academic Press Inc., London, 2<sup>nd</sup> edition.
- [14]. Sing K.S.W. (1995). Physisorption of nitrogen by porous materials. *Journal of porous materials*, 2(1): 5-8.

